

Improving Subgraph Matching by Combining Algorithms and Graph Neural Networks

Shuyang Guo

SKLCCSE, Beihang University
Beijing, China
guoshuyang@buaa.edu.cn

Ting Deng

SKLCCSE, Beihang University
Beijing, China
dengting@buaa.edu.cn

Xiangping Huang

TravelSky Technology Limited
Beijing Engineering Research
Center of Civil Aviation Big Data
Beijing, China
xphuang@travelsky.com.cn

Wenjin Xie

SKLCCSE, Beihang University
Beijing, China
xiewj@act.buaa.edu.cn

Richong Zhang

SKLCCSE, Beihang University
Beijing, China
zhangrc@act.buaa.edu.cn

Ping Lu*

SKLCCSE, Beihang University
Beijing, China
luping@buaa.edu.cn

Jianxin Li

SKLCCSE, Beihang University
Beijing, China
lijx@buaa.edu.cn

Zhongyi Liu

TravelSky Technology Limited
Beijing Engineering Research
Center of Civil Aviation Big Data
Beijing, China
liuzy@travelsky.com.cn

Abstract

Homomorphism is an important structure-preserving mapping between graphs. Given a graph G and a pattern Q , the subgraph homomorphism problem is to find a mapping φ from Q to G such that adjacent vertices of Q are mapped to adjacent vertices in G . Unlike the subgraph isomorphic mapping that is injective, homomorphism allows multiple vertices in Q to map to the same vertex in G , increasing complexity. We develop HFrame, the first GNN-based framework for subgraph homomorphism, by combining algorithms and machine learning. We show that HFrame is more expressive than the vanilla GNN, *i.e.*, HFrame can distinguish more graph pairs (Q, G) such that Q is not homomorphic to G . Moreover, we provide a generalization error bound for HFrame. Using real-life and synthetic graphs, we show that HFrame is up to $101.91\times$ faster than exact matching algorithms, and its average accuracy can reach 0.962.

CCS Concepts

- Computing methodologies → Neural networks; Model development and analysis.

Keywords

Graph Neural Network, Graph Matching, Expressive Power, Generalization Bound

*Corresponding author

Permission to make digital or hard copies of all or part of this work for personal or classroom use is granted without fee provided that copies are not made or distributed for profit or commercial advantage and that copies bear this notice and the full citation on the first page. Copyrights for components of this work owned by others than the author(s) must be honored. Abstracting with credit is permitted. To copy otherwise, or republish, to post on servers or to redistribute to lists, requires prior specific permission and/or a fee. Request permissions from permissions@acm.org.

KDD '25, Toronto, ON, Canada

© 2025 Copyright held by the owner/author(s). Publication rights licensed to ACM. ACM ISBN 979-8-4007-1454-2/2025/08
<https://doi.org/10.1145/3711896.3737006>

ACM Reference Format:

Shuyang Guo, Wenjin Xie, Ping Lu, Ting Deng, Richong Zhang, Jianxin Li, Xiangping Huang, and Zhongyi Liu. 2025. Improving Subgraph Matching by Combining Algorithms and Graph Neural Networks. In *Proceedings of the 31st ACM SIGKDD Conference on Knowledge Discovery and Data Mining V.2 (KDD '25), August 3–7, 2025, Toronto, ON, Canada*. ACM, New York, NY, USA, 12 pages. <https://doi.org/10.1145/3711896.3737006>

KDD Availability Link:

The source code of this paper has been made publicly available at <https://doi.org/10.5281/zenodo.15572826>.

1 Introduction

Pattern matching is to identify instances of a pattern Q in a graph G , and has received extensive interest across various fields, *e.g.*, discovering motifs in biology [20, 49, 67], finding experts in social networks [16, 30, 62], and reasoning on knowledge graph [48, 66, 78].

There exist two semantics for pattern matching, namely subgraph isomorphism and homomorphism. (1) The isomorphic semantics demands that the matched instances of Q in G (*i.e.*, a subgraph of G) must be the same as Q . This semantics has been widely studied, *e.g.*, discovering motifs from biological network [20, 49, 67]. (2) Homomorphic semantics, on the other hand, permits that Q can be “embedded” into the identified subgraph of G , *i.e.*, the subgraph can be deviated from Q . It has been widely used in graph query languages like Cypher [24] and SPARQL [57]. The difference between isomorphism and homomorphism lies in whether different vertices in Q can be mapped to the same vertex in G (see Section 2).

The graph pattern matching problem under isomorphic semantics has been extensively studied, leading to the development of many algorithms (*e.g.*, [9, 12–14, 41, 42, 44, 46, 65, 68, 80]; see [90] for a survey and comparison). All such algorithms work in the following steps: (1) establish a matching order $O = (u_1, \dots, u_n)$ for vertices in pattern Q ; (2) compute a set $C(u)$ of candidate matches for each pattern vertex u in Q , *e.g.*, $C(u)$ consists of all vertices in G that

have the same label with u ; (3) iteratively identify matches using $C(u)$ as follows: (a) select a candidate v_1 in $C(u_1)$ for the first vertex u_1 in the order O ; (b) from the neighbors u_2 of u_1 , find a candidate v_2 in $C(u_2)$ that has the same edge labels as u_2 in Q ; (c) continue these steps for all other vertices in Q , and check whether the selected candidates form a match of Q ; if not, backtrack to re-examine other vertices in $C(u_2)$. These techniques can be adapted to homomorphic semantics, except that the identified subgraphs of G are not required to be the same as Q in the last step. However, such algorithms take exponential runtime due to backtracking, and cannot efficiently handle large-scale graphs. To address this, various optimization strategies have been developed, including index structures to filter candidates [12, 41, 46], and dual simulation [53, 88] and 1-WL algorithms [17, 74] to approximate results. Despite these efforts, the algorithms still suffer from taking long time due to the high complexity.

Machine learning (ML), particularly Graph Neural Networks (GNNs), has been applied in the subgraph matching problem [47, 51, 58, 81, 83]. Such solutions work as follows: (1) exploit a GNN to compute the embedding for each vertex in Q and G , capturing the surrounding topological structures of the vertex; and (2) assessing subgraph matching by comparing these embeddings within the order-embedding space [83]. These algorithms are efficient, since they do not depend on backtracking. However, their predictions are not accurate, since their expressive power is bounded by the 1-WL algorithm [77], an approximate algorithm. Moreover, these models cannot directly handle homomorphic semantics, since they do not account for properties of homomorphic mappings, e.g., two distinct pattern vertices can be mapped to the same vertex in G , allowing two graphs with different sizes be homomorphic to each other.

Generalization error is an important property of machine learning models, reflecting how well they work on unseen inputs. Metrics for generalization error include Rademacher complexity [36] and VC dimension [55]. The Rademacher complexity of GNN models is established in [36]. However, no such bound exists for subgraph isomorphic or homomorphic mapping models.

In this paper, we aim to answer the following questions. (1) Can we integrate algorithmic solution with an ML-based techniques, to develop approximate framework for graph pattern matching under homomorphic semantics? (2) Does the proposed framework is more expressive than existing approximate solutions? And (3) what is the generalization error bound of the proposed framework?

Contribution. Our contributions are listed as follows.

(1) We introduce HFrame, a framework designed for the subgraph homomorphism problem. Given Q and G , it first leverages a PTIME algorithm DualSim [53] for graph dual simulation, to identify candidates set $C(u)$ for each vertex u in Q . Then it invokes an ML model HGIN to make predictions on these candidates. By combining algorithmic solutions and ML techniques, HGIN can deliver high-quality predictions, striking a balance between complexity and accuracy.

(2) We develop an ML model HGIN for subgraph homomorphism in HFrame, building upon IDGNN [84], which is tailored for subgraph isomorphism. Instead of using multisets to gather messages as in IDGNN, we adopt sets to gather embeddings and remove duplicate messages, since two vertices can be mapped to the same vertex in

homomorphism. We encode both directions and labels of edges into embeddings of vertices, to improve the accuracy of HGIN.

(3) We first show that HFrame is more expressive than existing models, and capable of distinguishing more non-homomorphic graphs. Then we provide the first generalization error bound for models addressing the subgraph homomorphism problem.

(4) We conducted extensive experiments on real-life and synthetic graphs, and found the following: (a) HFrame is efficient. It on average outperforms existing algorithms for subgraph homomorphism problems by up to 101.91 \times , and its accuracy on average is 0.962. (b) HFrame is effective. Its accuracy is at least 0.921 on all graphs, and is on average 21% higher than existing ML solutions. (c) HFrame performs well on unseen data. After HFrame is trained on synthetic graphs, its accuracy can reach 0.892, 0.874 and 0.872 on real-life graphs Citeseerx, IMDB and DBpedia, respectively.

Related work. We categorized the related work as follows.

Graph pattern matching algorithm. Algorithms for the subgraph isomorphism problem have been extensively studied. Ullmann proposed the first backtracking-based algorithm for subgraph isomorphism [68]. Subsequent research in algorithms for exact graph pattern matching focuses on developing pruning methods [18, 19] and improving index structures [12, 64, 79, 91], and so on.

Isomorphic mappings suffer from two major drawbacks: (1) the decision version of subgraph isomorphism is NP-complete [23], and (2) the requirement of injective mapping could be too strict in many cases, especially when the data source is noisy [85]. To address these challenges, (1) a series of studies focus on designing similarity functions and deriving matching results through top- k candidates or the establishment of a similarity threshold [22, 26, 28, 45, 76, 92]. (2) The other studies relax the injective map to less restrictive relations. Bounded simulation is developed to bound the lengths of matching paths [27]. Dual simulation and strong simulation are proposed in [52] to bound directions of edges and distances of vertices in a match, respectively. Subsequently, various simulation-based matching algorithms have been developed [25, 31–33, 35].

ML Models for graph pattern matching. Multiple ML models are developed for graph pattern matching [47, 51, 58, 81, 83]. Most of these models are based on Graph Neural Networks (GNNs), to compute embeddings of vertices in a graph [59], and make a prediction using the order-embedding space [83] or MLP [51]. Most work focus on enhancing GNNs architecture [15, 34, 70, 72, 89], to learn more topological information. Zhang et al. [86] encoded distance information into vertex embeddings. Geerts et al. [37] proposed a model to aggregate information from k -order neighbors using computational operators. You et al. [84] injected a unique color identity to nodes, and performed heterogeneous message passing to obtain the embedding. Xu et al. [77] optimized the aggregation function by using multisets, to generate distinct embeddings for different nodes. Maron et al. [54] proposed a model consisting of both equivariant linear layers and nonlinear activation layers.

There has also been work on studying properties of GNNs. (1) The expressive power of these GNN models can be bounded by the Weisfeiler-Lehman (WL) hierarchy [10, 56, 77, 86, 87], descriptive complexity [39], fragments of FO logic [11] and global feature

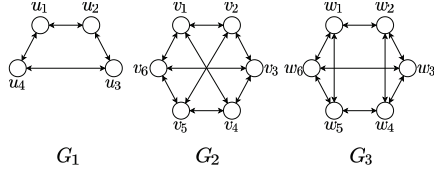


Figure 1: Differences between Iso and Hom

map transformer [38]; see [86] for a recent survey. (2) The generalization error bound for GNNs can be measured by Rademacher complexity [36], VC dimension [55] and generalization gap [73, 73].

2 Preliminaries

Let Γ be a countably infinite set of labels.

Graphs. Consider directed labeled graphs $G = (V, E, L)$, where (1) V is a finite set of vertices; (2) $E \subseteq V \times \Gamma \times V$ is a finite set of edges, where $\langle v_1, r, v_2 \rangle$ is an edge from v_1 to v_2 , carrying label $r \in \Gamma$; and (3) L is a labeling function that assigns a label $L(v) \in \Gamma$ to each vertex v in V . Let R_G be the set of all edge labels in G .

For each vertex $u \in V$, denote by $N_r^+(u)$ (resp. $N_r^-(u)$) the set of its *outgoing* (resp. *incoming*) neighbors u_1 of u that have an edge labeled r from u to u_1 (resp. from u_1 to u). That is, $N_r^+(u) = \{u_1 \mid \langle u, r, u_1 \rangle \in E\}$ and $N_r^-(u) = \{u_1 \mid \langle u_1, r, u \rangle \in E\}$. Denote by $N(u)$ the set of all neighbors of u , i.e., $N(u) = \bigcup_{r \in R_G} (N_r^-(u) \cup N_r^+(u))$.

Isomorphism (Iso) and homomorphism (Hom). We introduce the semantics of subgraph isomorphism and homomorphism. Consider a pattern $Q = (V_Q, E_Q, L_Q)$ and a graph $G = (V_G, E_G, L_G)$. Here, a pattern is also a directed labeled graph.

Subgraph isomorphism. An *isomorphic mapping* from Q to G , denoted by $Q \sqsubseteq G$ is an injective mapping φ from V_Q to V_G such that (1) for each $u \in V_Q$, u and $\varphi(u)$ carry the same label, i.e., $L_Q(u) = L_G(\varphi(u))$; and (2) the adjacency relation preserves, i.e., $\langle u, r, u' \rangle \in E_Q$ if and only if $\langle \varphi(u), r, \varphi(u') \rangle \in E_G$. When such an injective mapping φ exists, we say that Q is subgraph isomorphic to G .

Subgraph homomorphism. A *homomorphic mapping* from Q to G , denoted by $Q \triangleright G$, is a mapping φ from V_Q to V_G such that (1) for each $u \in V_Q$, u and $\varphi(u)$ carry the same label, i.e., $L_Q(u) = L_G(\varphi(u))$; and (2) when there is an edge $\langle u, r, u' \rangle$ in E_Q , edge $\langle \varphi(u), r, \varphi(u') \rangle$ exists in E_G . Observe that (a) φ may not be injective; and (b) when $\langle \varphi(u), r, \varphi(u') \rangle \in E_G$, $\langle u, r, u' \rangle$ may not exist in E_Q . When such a mapping φ exists, we say that Q is subgraph homomorphic to G .

Differences. Since subgraph isomorphism requires that the mapping φ is injective, it has the anti-symmetry property, i.e., for two graphs G and H , if $G \sqsubseteq H$ and $H \sqsubseteq G$, then G and H are the same graph. However, subgraph homomorphism does not have this property. That is, there exist two distinct graphs G and H such that $G \triangleright H$ and $H \triangleright G$.

Example 2.1. Consider graphs G_1 and G_2 in Figure 1. Assume that all vertices (resp.edges) in G_1 and G_2 carry the same label. Observe that (a) G_1 is subgraph homomorphic and subgraph isomorphic to G_2 via mapping $\varphi_1(u_i) = v_i$ ($i=1, 2, 3, 4$); (b) G_2 is not subgraph isomorphic to G_1 , since G_2 has more vertices than G_1 ; and (c) G_2 is subgraph homomorphic to G_1 via mapping $\varphi_2(v_i) = u_i$ ($i=1, 2, 3, 4$), $\varphi_2(v_5) = u_3$ and $\varphi_2(v_6) = u_2$. That is, G_1 and G_2 are subgraph homomorphic to each other, but they have different numbers of vertices.

Due to such differences, solutions for subgraph isomorphism and homomorphism are distinct (see Section 3).

Problem definition. The paper studies the following subgraph homomorphism problem, denoted by SHP: *given a pattern Q and a graph G , whether there exists a homomorphic mapping φ from Q to G .*

Remark. Such decision problem can be applied in the following scenarios: (1) frequent pattern mining [82] and graph pattern dependency discovery [29], where pattern quality is usually determined by the number of vertices matching the pivot (i.e., a designated vertex) of Q , which can be computed by determining *the existence of matches* on these vertices, rather than enumerating the matches; (2) querying for key vertices satisfying some properties defined by patterns, e.g., a SPARQL query from Wikidata [8] to find articles on Punjabi Wikipedia about Pakistani actresses, which can be modeled as a pattern with Articles as the pivot; and (3) accelerating enumerations by filtering candidates with the decision problem and inducing a smaller subgraph before enumeration (see Section 5).

Existing solutions. In this paper, we develop an approximate solution for SHP. There exist two categories of approximate solutions, i.e., algorithmic approximations and machine learning based solutions. We aim to combine these two solutions to develop a more accurate solution. We first present the two existing solutions.

Dual Simulation. Given a pattern $Q = (V_Q, E_Q, L_Q)$ and a graph $G = (V_G, E_G, L_G)$, it is to compute a matching relation $S_{(Q,G)}$ of vertex pairs (u, v) where $u \in V_Q$ and $v \in V_G$, such that u and v have the same neighbors. Using $S_{(Q,G)}$, we can approximate the subgraph homomorphic problem by checking whether $(u, v) \in S_{(Q,G)}$.

The relation $S_{(Q,G)} \subseteq V_Q \times V_G$ is defined as follows: (1) for each $(u, v) \in S_{(Q,G)}$, $L_Q(u) = L_G(v)$; and (2) for each $u \in V_Q$, there exists $v \in V_G$ such that (i) $(u, v) \in S_{(Q,G)}$; (ii) for each outgoing edge (u, u_1) in E_Q , there is an outgoing edge (v, v_1) in E_G with $(u_1, v_1) \in S_{(Q,G)}$; and (iii) for each incoming edge (u_2, u) in E_Q , there is an incoming edge (v_2, v) in E_G with $(u_2, v_2) \in S_{(Q,G)}$.

The relation $S_{(Q,G)}$ can be computed in $O((|V_Q| + |E_Q|)(|V_G| + |E_G|))$ time via algorithm DualSim [53] presented in Figure 2. Intuitively, for each vertex u in Q , it first initializes the set $C(u)$ with vertices in G carrying the same label as u (lines 1); then it iteratively removes a candidate v from $C(u)$, if v does not have the same incoming edges (lines 3-5) or the same outgoing edges (lines 6-8) as vertex u in Q . It repeats these steps for T times (line 2).

Remarks. The number T is bounded by $O((|V_Q| + |E_Q|)(|V_G| + |E_G|))$ [53]. However, only a few fixed iterations suffice to filter candidates [41]. We set $T = 2$ in the experiments (see Section 5).

Graph Neural Networks (GNNs). Given a graph G , a pattern Q and two vertices u and v from Q and G , respectively, GNN-based solution checks the existence of homomorphic mapping as follows [69, 83]: (1) compute the embeddings of u and v using GNNs; let $h_u = (a_1, \dots, a_d)$ and $h_v = (b_1, \dots, b_d)$ be the embeddings of u and v , respectively; and (2) exploit the order embedding space to check the existence of homomorphic mappings, i.e., a homomorphic mapping φ exists if and only if $a_i \leq b_i$ for all $i \in [1, d]$.

To compute the embeddings of vertices, we can adopt the identity-aware GNN (IDGNN) [84], since IDGNN is more expressive than vanilla GNN [84]. Given a graph G and a vertex u , IDGNN computes

Input: A graph G , a pattern Q and a number T .
Output: The maximum match relation $S_{(Q,G)}$ in G for Q .

1. set $C(u) := \{v \mid v \in V_G \wedge L_Q(u) = L_G(v)\}$ for each u in V_Q ;
2. **for each** $i \in [1, T]$ **do**
3. **for each** $e = (u, u') \in E_Q$ and $v \in C(u)$ **do**
4. **if** no edge (v, v') in G with $v' \in C(u')$ **then**
5. $C(u) := C(u) \setminus \{v\}$;
6. **for each** $e = (u', u) \in E_Q$ and $v \in C(u)$ **do**
7. **if** no edge (v', v) in G with $v' \in C(u')$ **then**
8. $C(u) := C \setminus \{v\}$;
9. $S_{(Q,G)} := \{(u, v) \mid u \in V_Q, v \in C(u)\}$;
10. **return** $S_{(Q,G)}$;

Figure 2: Algorithm DualSim

a d -dimensional vector to represent u in G by iteratively aggregating information collected from its neighbors. More specifically, (1) IDGNN first constructs the k -hop ego network G_u centered at u , *i.e.*, the subgraph induced by the k -hop neighbors of u ; (2) next it computes the initial embedding of each vertex v in G_u using features of v , *e.g.*, the label of v ; (3) then it iteratively updates embeddings of all vertices in G_u as follows: (a) collect embeddings of neighbors of a vertex v in G_u ; and (b) transform the received embeddings via message-passing functions; that is, let v_1, \dots, v_n be the neighbors of vertex v ; the message-passing function for the embedding of v_i is MSG_1 if $v_i = u$; otherwise the message-passing function is MSG_0 . This step is repeated for m times. Note that (i) the ego network G_u is used to compute the embedding of center u only; and (ii) parameter m is also called the number of the layers in IDGNN.

Remark. These two approximate solutions have their pros and cons.

(1) DualSim can process any given patterns and graphs, no matter whether they have been inspected before or not; moreover, it ensures that all matches can be returned, *i.e.*, the recall of DualSim is 1; but it may return extra results, *i.e.*, it will return false positive answer. Consider graphs G_2 and G_3 in Figure 1. There does not exist a homomorphic mapping from G_3 to G_2 , since G_3 contains triangles, but G_2 does not. However, $S_{(G_2, G_3)} = V_{G_2} \times V_{G_3}$, *i.e.*, $(v_i, w_j) \in S_{(Q,G)}$, $i, j \in [1, 6]$. See the proof of Theorem 4.2 for more details.

(2) GNN models can achieve good accuracy in performing tasks like node classification [43], recommendation system [61] and anomaly detection [71], and can become more expressive using more information in the graphs [50, 51]. Moreover, the computation of GNNs are efficient, since it only exploits neighbors of a vertex to make a prediction. The computation can be further accelerated using sampling techniques when processing large-scale graphs [40]. But GNN models may return error prediction, and miss some matches.

3 Framework for homomorphic mapping

We provide HFrame, a framework for the subgraph homomorphic problem, by integrating algorithms and machine learning models. The framework is outlined in Figure 3. Intuitively, the combination of DualSim and HGIN in HFrame enhances the efficiency and accuracy of the predictions due to the following mechanisms. (1) DualSim removes irrelevant information from graph G , which boosts the performance of HGIN by focusing only on essential data. (2) HGIN optimizes the prediction by computing only embeddings of vertices, rather than embeddings of patterns and graphs.

In this way, HGIN can leverage the locality of subgraph matching, *i.e.*, HGIN only inspects a small neighborhood of each vertex, which reduces the complexity of HGIN and improves the accuracy of HFrame. (3) HGIN only verifies candidates of the pivot u_p of Q , since when Q is homomorphic to G , the pivot u_p must be mapped to some vertex in G . The selection of pivot u_p can be based on the degrees of vertices, *e.g.*, picking the vertex with the maximum degree in Q [81].

Homomorphic Neural Node Matching (HGIN). It is to decide, given a pattern Q , a graph G , vertex u in Q and vertex v in G , whether there is a homomorphic mapping φ from Q to G such that $\varphi(u) = v$.

Overview. We design HGIN by extending IDGNN [84], to address the following three challenges from homomorphic semantics.

(1) We need to ensure that two distinct vertices in Q can be mapped to the same vertex in G . We illustrate two such scenarios in Figure 4.

(a) Consider pattern Q_1 and graph G_4 in Figure 4. Assume that all vertices and edges in Q_1 and G_4 have the same label. There is a homomorphic mapping φ_1 from Q_1 to G_4 as follows: $\varphi_1(u_1) = v_1$, $\varphi_1(u_2) = h_1(u_3) = v_2$. Note that u_2 and u_3 are both mapped to v_2 in h_1 .

To handle such case with GNNs, we use *sets* to store received embeddings of neighbors, rather than multisets as in IDGNN. In this way, when embeddings of u_2 and u_3 are the same, the duplicated one will be removed, and only embedding of u_2 or u_3 is used. As a result, the embeddings of u_1 in Q_1 and vertex v_1 in G_1 are the same, from which HGIN predicts that Q_1 is homomorphic to G_4 .

(b) Consider Q_2 and G_5 in Figure 4, which are two cycles of length 6 and 3, respectively, and all vertices and edges carry the same label. There exists a homomorphic mapping φ_2 from Q_2 to G_5 as follows: $\varphi_2(u_1) = \varphi_2(u_4) = v_1$, $\varphi_2(u_2) = \varphi_2(u_5) = v_2$ and $\varphi_2(u_3) = \varphi_2(u_6) = v_3$. However, IDGNN can only distinguish the two graphs, and cannot verify the existence of such a mapping, since MSG_1 and MSG_0 is not comparable. To address this, we introduce the following two extensions. (a) We enforce that MSG_1 is sufficiently larger than MSG_0 when training HGIN. (b) We compute a set \mathcal{L}_Q of lengths of cycles that contain u_1 in pattern Q , and use MSG_1 only when vertex v_1 also appears in a cycle of length l in G satisfying that $l \in \mathcal{L}_Q$.

To show the effectiveness, consider the following two cases.

(i) When pattern Q contains a cycle of length l involving u , whereas graph G does not have such a cycle involving v , the computation of u 's embedding in Q invokes MSG_1 more frequently. Since MSG_1 is sufficiently larger than MSG_0 , the embedding of u is larger than that of v , indicating that no homomorphic mapping from Q to G exists.

(ii) Conversely, if G contains a cycle of length l involving v , whereas Q does not, MSG_0 is invoked for vertices within the cycle of length l in both Q and G , which cannot result in that the embedding of u is larger than that of v , thus retaining the semantics of homomorphic mappings. Given Q_2 and G_5 in Fig. 4, although G_5 contains a cycle of length 3 involving v_1 , whereas Q_2 does not have such a cycle involving u_1 , MSG_0 is invoked to compute embeddings for both Q_2 and G_5 .

(2) Since IDGNN does not support edge labels, and cannot be directly used on the homomorphism problem, we extend the R-GCN framework [60]. The extension introduces a relation-specific transformation, to accommodate edge labels. More specifically, we categorize edges by their labels, and assign different weights to different

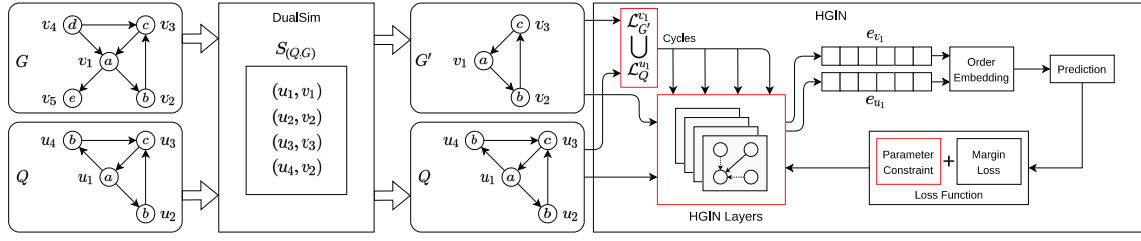


Figure 3: The framework of HFrame. (1) It first computes $S_{(Q,G)}$ via DualSim, to filter candidate sets $C(u)$ for each vertex u in Q , and construct a subgraph G' by removing irrelevant vertices and edges from G ; (2) it then generates embeddings of vertices via HGIN; and (3) it finally makes a prediction via the order embedding space. Its novelties (marked red) consist of (a) adopting sets to collect messages, (b) using cycles to select message-passing functions, and (c) integrating parameters into the loss function.

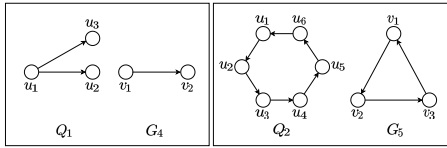


Figure 4: Cases for homomorphism

labels. To address the directions of edges, we compute the embeddings with incoming edges and outgoing edges separately. Then we concatenate these embeddings to form the embedding of vertices.

(3) HGIN utilizes the order-embedding space to check the existence of homomorphic mappings [83], involving comparison of values at each index of the embeddings. However, the computed embeddings of vertices might include negative values. To overcome this, we normalize the embeddings, to ensure that all values are positive.

Putting these together, we present HGIN in Figure 3.

Embeddings of Q . Given a vertex u , it first constructs a subgraph Q_u of Q , induced by the m -hop neighbors of u , where m is a pre-defined parameter; then it iteratively computes the embedding of each vertex u_c in Q_u as follows: (a) collects the embeddings of u_c 's neighbors via a message passing function, and updates u_c 's embedding using the collected embeddings via an aggregation function. More specifically, it computes the embedding of u_c as follows:

$$h_{u_c}^0 = e_x^f \quad (1)$$

$$h_{u_c,i}^k = \text{AGG}^k \left(\sum_{r \in R_G} \text{MSG}_{1[u_n=u]}^{k,r} (\{h_{u_c}^{k-1}, u_n \in N_r^-(u_c)\}), h_{u_c}^{k-1} \right) \quad (2)$$

$$h_{u_c,o}^k = \text{AGG}^k \left(\sum_{r \in R_G} \text{MSG}_{1[u_n=u]}^{k,r} (\{h_{u_c}^{k-1}, u_n \in N_r^+(u_c)\}), h_{u_c}^{k-1} \right) \quad (3)$$

$$h_{u_c}^k = \text{COM}(h_{u_c,i}^k, h_{u_c,o}^k). \quad (4)$$

Here, (1) $N_r^-(u_c)$ (resp. $N_r^+(u_c)$) is the set of neighbors of u_c which have an outgoing edge to u_c (resp. an incoming edge from u_c) labeled r ; and (2) the message passing function $\text{MSG}_{1[u_n=u]}^{k,r}$ collects and transforms embeddings of neighbors of u_c ; in this paper, we adopt matrix multiplication as the message passing functions; more specifically, $\text{MSG}_{1[u_n=u]}^{k,r}(N_r^-)$ transforms the message to

$$\sum_{u_n \in N_r^-} W_{1[u_n=u]}^{k,r} h_{u_n}^{k-1}; \quad (5)$$

here N_r^- is the set of outgoing neighbors; the message passing functions for incoming neighbors are defined similarly; (3) $1[u_n=u]$ is an indicator function that returns 1 if u_n and u are the same vertex, and 0 otherwise; that is, if the neighbor u_n is the center vertex u

of Q_u , then the message passing function is $\text{MSG}_1^{k,r}$; otherwise, the message passing function is $\text{MSG}_0^{k,r}$; (4) AGG^k combines the embeddings of neighbors and the current embedding of u_c as follows:

$$\text{AGG}^k(\text{MSG}, e_2) = W_1 e_2 + \text{MSG}; \quad (6)$$

and (5) COM updates the embedding of u_c by concatenating the embeddings of its incoming neighbors and outgoing neighbors.

Embeddings of G . For a pattern Q and a graph G , given vertices u in Q and v in G , it first compute the sets \mathcal{L}_Q^u and \mathcal{L}_G^v of all cycles of length l in Q and G containing u and v , respectively, where l is bounded by m , i.e., the number of layers in HGIN. Let G_v be the subgraph of G , induced by the m -hop neighbors of v . Then it iteratively computes the embedding of each vertex v_c in G_v in the same way as it does for embedding Q , except that the message-passing functions for each neighbor v_n of vertex v_c in G_v is $\text{MSG}_{1[v_n=v][k \in \mathcal{L}_Q^u]}^{k,r}$. Here $1[v_n=v][k \in \mathcal{L}_Q^u]$ is a Boolean function, which returns 1 when (1) the neighbor v_n is the center v of G_v , and (2) Q has a cycle of length k containing the center u in Q_u , and 0 otherwise.

Note that when Q_u does not have a cycle of length k that contains the center u , the message-passing function is $\text{MSG}_0^{k,r}$, regardless of whether v_n is the center v of G_v or not.

Normalization. After HGIN generates embeddings of vertices, it conducts L2 normalization to ensure that all embeddings are positive. More specifically, for each vertex v , let $e_v = (x_1, \dots, x_d)$ be its embedding generated via HGIN, and its L2 norm is $\|e_v\|_2 = \sqrt{x_1^2 + \dots + x_d^2}$. Then the normalized embedding e_v^N of the original embedding e_v is defined as $e_v^N := \frac{|e_v|}{\|e_v\|_2}$.

Prediction Function. Given the embedding $e_u = (a_1, \dots, a_d)$ of vertex u in Q and the embedding $e_v = (b_1, \dots, b_d)$ of v in G , it exploits the order embedding space [69, 83], to check the existence of homomorphic mapping from Q to G as follows: Q is homomorphic to G if and only if $a_i \leq b_i$ for all $i \in [1, d]$. To improve the generalization of HGIN, a threshold t is used to bound the distance between e_u and e_v . More specifically, the prediction function f is defined as:

$$f(e_u, e_v) = \begin{cases} 1 & \text{if } \mathcal{M}(e_u, e_v) \leq t; \\ 0 & \text{otherwise.} \end{cases} \quad (7)$$

Here, function $\mathcal{M}(e_u, e_v)$ is defined as $\|\max(0, e_u - e_v)\|_2^2$.

Loss function. To train HGIN, we enhance the max-margin loss function by integrating message-passing functions. This enforces vertex identities in IDGNN, by ensuring that $M_1^{k,r}$ is sufficiently larger than $M_0^{k,r}$. When Q has a cycle of length l containing u , but G does not have such a cycle containing v , computing the embedding of u invokes message-passing functions $M_1^{k,r}$ more frequently than computing the embedding of v . Thus, the embedding of u is larger than that of v , implying that Q is not homomorphic to G . More specifically, the max-margin loss function is defined as follows.

$$\begin{aligned} \mathcal{L} = & \sum_{(Q,u,G,v) \in P} (\mathcal{M}(h_u, h_v) - \alpha) \\ & + \sum_{(Q,u,G,v) \in N} \max\{0, \alpha - \mathcal{M}(h_u, h_v)\} \\ & + \sum_{k \leq m} \sum_{r \in R} \frac{1}{\text{MSG}_1^{k,r} - \text{MSG}_0^{k,r}}, \end{aligned} \quad (8)$$

where (1) P is the set of positive examples (Q, u, G, v) such that there exists a homomorphic mapping φ from Q to G such that $\varphi(u) = v$, (2) N is the set of negative examples (Q, u, G, v) such that there does not exist a homomorphic mapping φ from Q to G such that $\varphi(u) = v$, and (3) α is the margin threshold for the prediction function.

Remark. The loss function \mathcal{L} differs from the loss function for subgraph matching in [83] as follows.

(1) We add the term $\frac{1}{\text{MSG}_1^{k,r} - \text{MSG}_0^{k,r}}$ to ensure that $\text{MSG}_1^{k,r}$ is sufficiently larger than $\text{MSG}_0^{k,r}$ for each edge label r . Intuitively, sufficiently large $\text{MSG}_1^{k,r}$ allocates more weights to the appearance of center vertices. Combining with the set C of cycle sizes, HFrame can distinguish more negative pairs than existing solutions, i.e., HFrame has more expressive power (see Section 4).

(2) We add the term $-\alpha$ to penalize errors incurred by positive training data. This guarantees that the loss function is 1-Lipschitz, which is used to prove the generalization bound for HFrame (Theorem 4.4).

Complexity. HFrame takes $O(|Q||G| + m\delta_{\max}(|Q| + |G|)(f(|Q|) + f(|G|)))$ time and $O(m\delta_{\max}d(|G| + |Q|)f_M)$ space for inference, and $O((|P| + |N|)(|Q||G| + m\delta_{\max}(|Q| + |G|)(f(|Q|) + f(|G|))))$ time and $O((|P| + |N|)m\delta_{\max}d(|G| + |Q|)f_M)$ space for training. Here (1) m is number of layers, (2) δ_{\max} is the maximum degree of Q and G , (3) f is a lower-degree polynomial denoting embedding time, (4) d is dimension of embeddings, (4) f_M is the size of HGIN, and (5) $|P|$ (resp. $|N|$) is the number of positive (resp. negative) training data.

4 Theoretical analysis

We first study the expressive power of HFrame and then establish a generalization error bound for it. Since HFrame consists of DualSim and HGIN, we start with comparing their expressive power, to justify their combination. See Appendix for detailed proofs.

(1) Expressive power. We consider the following three cases.

(a) DualSim vs. vanilla HGIN. We first show that DualSim provides an upper bound for the expressive power of vanilla HGIN (HGIN^v), which uses a unified message passing function for all vertices. More specifically, the same message passing function $\text{MSG}^{k,r}$ is applied

to all neighbors of vertices. Intuitively, both HGIN^v and DualSim inspect only neighbors of a vertex, and have similar expressive power. We prove that there exists a HGIN^v that is as expressive as DualSim.

THEOREM 4.1. *Given a pattern Q , a graph G , a vertex u in Q and a vertex v in G , if HGIN^v returns false, then $(u, v) \notin S_{(Q,G)}$, i.e., DualSim also determines that there exists no homomorphism mapping φ from Q to G such that $\varphi(u) = v$, even when all functions $\text{MSG}^{k,r}$ and AGG^k ($k \leq m$) in HGIN^v are injective and monotonic.*

PROOF. We prove it by contradiction. Assume by contradiction that there exist a pattern Q , a graph G , a vertex u in Q and a vertex v in G , such that HGIN^v returns false, but DualSim returns true, i.e., $(u, v) \in S_{(Q,G)}$. We deduce a contradiction as follows. (a) Computing embeddings of u and v can be represented by trees of height m , where m is the number of layers in HGIN^v. (b) Because $\text{MSG}^{k,r}$ and AGG^k ($k \leq m$) in HGIN^v are injective and monotonic, there exists a path p_0 in the computation tree for u such that no path from v carries the same labels as p_0 . However, if these hold, DualSim can also identify such path and return false, a contradiction. \square

(b) DualSim vs. HGIN. When HGIN uses different message passing functions for vertices, it can distinguish the center from other vertices and has a higher expressive power than DualSim.

THEOREM 4.2. *HGIN is more expressive than DualSim.*

PROOF. (1) We first show that given a pattern Q , a graph G , a vertex u in Q and a vertex v in G , when DualSim returns false, i.e., $(u, v) \notin S_{(Q,G)}$, there is a HGIN that returns false given the input.

(2) We next show that HGIN can distinguish more graphs than DualSim. Consider graphs G_2 and G_3 in Figure 1, extended from [84]. (a) There is no homomorphic mapping from G_3 to G_2 , since G_3 contains triangles while G_2 does not. (b) HGIN returns false given w_1 and v_1 , since w_1 is in a cycle of length 3 while v_1 does not, which results in a larger embedding of w_1 than that of v_1 . (c) DualSim confirms that $(w_1, v_1) \in S_{(G_3, G_2)}$, since G_2 and G_3 are regular, all vertices have similar neighborhoods, and $S_{(G_3, G_2)} = V_{G_3} \times V_{G_2}$. \square

(c) DualSim vs. HGIN of finite dimensions. HGIN represents vertices with embeddings of finite dimensions. For graphs with a large number of labels (e.g., more edge labels than the embedding dimension), we can construct a pattern Q and a graph G with different label sets such that (1) the embedding of Q is smaller than that of G , but (2) Q is not homomorphic to G . However, DualSim can distinguish graphs with any number of labels, by directly comparing their labels.

THEOREM 4.3. *When the dimension of embeddings is finite, there exist two graphs that DualSim can distinguish, but HGIN cannot.*

PROOF. Assume that HGIN generates d -dimensional embeddings. (a) We select $2d$ distinct labels from the label set Γ and compute their embeddings using HGIN; then we choose d embeddings e_1, \dots, e_d such that each e_i has the maximum i -th element. (b) We construct a star pattern Q_s centered at v , with d edges, each labeled with one of the d picked labels. We then deduce a contradiction by comparing the embeddings of Q_s with that of the $2d$ distinct labels. \square

Theorems 4.2 and 4.3 imply that HGIN and DualSim have incomparable expressive power with finite embedding dimensions. We can improve pattern matching by combining DualSim with HGIN.

(2) Generalization bound. We give a generalization error bound for HFrame to measure its prediction accuracy on unseen data.

THEOREM 4.4. *The empirical Rademacher complexity of HFrame is $\hat{\mathcal{R}}(\mathcal{T}) \leq \frac{8}{N_T} + \frac{12}{\sqrt{N_T}} \sqrt{2|R|d^2 \log T}$, where \mathcal{T} maps the training data to its loss, and $T = 16M\sqrt{N_T d} \max\{B_x B_1, \mathcal{R}B_2\}$.*

Here, (1) $|R|$ is the number of edge labels in Q and G ; (2) N_T is the size of training data; and (3) M and \mathcal{R} are numbers determined by functions in HGIN. Assume that the norms of W_1 , $W_i^{k,r}$ and h_{uc}^k are bounded by B_1 , B_r and B_x , respectively.

Remark. We extend the proof of the Rademacher complexity for GNNs in [36]. (1) HFrame takes a pattern Q and a graph G as input, while GNNs in [36] process only one graph; (2) HFrame handles patterns and graphs with both labels and directions, which are not explored in [36]; (3) HGIN uses distinct message-passing functions for different neighbors, a feature absent in GNNs of [36]; (4) HGIN uses the max-margin loss function to compare embeddings of vertices, which complicates the analysis of HGIN.

5 Experimental study

Using real-life and synthetic graphs, we evaluated the (1) effectiveness, (2) efficiency, (3) parameter sensitiveness and (4) generalization of the proposed framework HFrame. (5) We also conducted an ablation study on HFrame, and (6) applied HFrame in subgraph homomorphism enumeration and frequent pattern mining.

Experimental settings. We start with the settings.

Data Graphs. We used six real-life graphs: (1) Citation, a citation network with 1,397,240 vertices and 3,016,539 edges, carrying 16,415 labels [1]; (2) Citeseerx, another citation network with 6,540,401 vertices and 15,011,260 edges, carrying 984 labels [2]; (3) DBLP, a collaboration network with 205,783 vertices and 301,561 edges, carrying 11 labels [3]; (4) IMDB, a movie database modeled as graph, with 5,101,080 vertices and 5,174,035 edges, carrying 38 labels [5]; (5) DBpedia, a knowledge graph with 5,174,170 vertices and 17,494,747 edges with 9,591 labels [4]; and (6) YAGO, a knowledge graph with 3,489,226 vertices and 7,351,194 edges carrying 15 labels [6].

For synthetic dataset, we generated a graph $G = (V, E, L)$, controlled by the number of vertices $|V|$ (up to 20M), the number of edges $|E|$ (up to 40M) and the number of labels $|L|$ (up to 500).

Baselines. We categorized the baselines as follows.

Algorithms. We compared HFrame with the following algorithms for subgraph matching: (1) the edge-join approach (EJ) [21], which computes the occurrences for each edge of the query in the data graph, finds an optimized plan to join these binary relations, and finally evaluates the query following the plan; (2) the path-join approach (PJ) [63], which first generates solutions to each root-to-leaf path of the given query, and then produces the answer by joining solutions of these paths; (3) SIM-TD [75], which encodes all possible homomorphisms from a pattern to the graph with the concept of answer graph; (4) a pattern matching algorithm DualSim [52] (see Section 2); and (5) popular graph DBMS Neo4j [7].

Among these algorithms, EJ, PJ, SIM-TD and Neo4j are exact algorithms, and DualSim is an approximate algorithm. For a fair comparison, we modified EJ, PJ, SIM-TD and Neo4j to return only one match, as we focus on decision problem rather than enumeration.

ML models. We compared with the following ML models: (6) NeuroMatch [83], which applies GNN to compute the embedding, and exploits the order embedding space to make predictions for subgraph isomorphism; (7) D2Match [51], which proposes a degeneracy procedure that frames subgraph matching as a subtree matching problem; and (8) DMPNN [50], which develops dual message passing neural networks to improve substructure representation.

Training data. We constructed training data by sampling from large data graphs following [51, 83]. It consists of both positive and negative data. (1) We constructed a set P of positive data (Q_p, u, G_p, v) , *i.e.*, there exists a homomorphic mapping φ from Q_p to G_p such that $\varphi(u) = v$. For each graph G , we (a) first randomly extract a subgraph G_p by performing BFS from a random vertex on G in 5 to 10 steps, (b) select a connected graph Q_p from G_p as the pattern, where the number of nodes in Q_p is between 3 and 20, (c) randomly copy vertices and edges in Q_p to enforce the homomorphic semantics, and (d) pick one vertex u from Q_p as the pivot and set the same vertex in G_p as the pivot v . (2) We also construct a set N of *negative data* (Q_n, u, G_n, v) , such that no homomorphic mapping exists from u to v . To this end, we first extract positive data (Q_p, u, G_p, v) as above, and then calibrate the pattern Q_p to create pattern Q_n that has no match in G_p , by adding edges randomly to Q_p or perturbing the pivot in G_p .

To make sure that HFrame is robust, we set the ratio of positive to negative instances as 1 : 3. Moreover, we employed Neo4j to compute the ground-truth between the patterns and the graphs.

We sampled 20,000 pairs of query and subgraph from each graph, *i.e.*, 5,000 positive and 15,000 negative examples, and split each dataset into training, validation and test sets at a ratio of 8:1:1. As EJ, PJ and D2Match do not support edge labels, when comparing with these baselines, we removed all edge labels from patterns and graphs for fair comparison. It should be noted that, since SIM-TD is only applicable to tree structure, every query was decomposed into multiple tree queries before conducting the experiments on SIM-TD.

Evaluation Metric. We tested accuracy of HFrame with the metric: $\text{Acc} = (TP + TN) / (TP + TN + FP + FN)$, where TP , TN , FP and FN denote the numbers of true positives, true negatives, false positives and false negatives, respectively. In terms of efficiency, we measure the end-to-end CPU time for exact algorithms (*i.e.*, EJ, PJ, SIM-TD and Neo4j); for HFrame, we measure CPU time for DualSim and GPU time for HGIN. When there exists no matching for a query, the exact algorithms will exhaustively traverse the entire search space before returning false. To ensure the fairness on efficiency comparison, we imposed a 30-second time limit on the runtime.

Experiment Environments. We run the experiments on a server running Ubuntu 11.4.0 with Intel Xeon E5-2680v4 CPU, NVIDIA Tesla V100 PCIe 32GB GPU and 512GB RAM. HGIN training and inference are performed on GPU, while the remaining components of HFrame run on CPU. By default, we set the number of layers $m = 5$, the dimension of embeddings $d = 64$, the margin $\alpha = 1.5$ and the threshold $t = 0.1$. We set the number of iterations for DualSim to 2. We ran each test 5 times, and report the average here.

Table 1: Accuracy Comparison Results (Acc)

Method	Citation	Citeseerx	DBLP	IMDB	DBpedia	YAGO	Synthetic
DualSim	0.669	0.573	0.674	0.590	0.601	0.575	0.692
NeuroMatch	0.804	0.803	0.837	0.798	0.782	0.783	0.857
D2Match	0.804	OOM	0.833	0.784	OOM	0.881	
DMPNN	0.815	0.812	0.842	0.806	0.805	0.794	0.889
HFrame	0.954	0.982	0.969	0.963	0.969	0.921	0.974
HFrameWS	0.895	0.952	0.965	0.961	0.941	0.902	0.939
HFrame _{MS}	0.837	0.826	0.838	0.812	0.805	0.788	0.883
HFrame _{WD}	0.888	0.950	0.926	0.919	0.866	0.855	0.929
HFrame _{WN}	0.938	0.963	0.952	0.950	0.918	0.893	0.951
HFrame _{WC}	0.930	0.920	0.945	0.937	0.921	0.884	0.942
HFrame _{WG}	0.943	0.950	0.957	0.946	0.944	0.899	0.965

Table 2: Efficiency Comparison results (Time in s/query)

Method	Citation	Citeseerx	DBLP	IMDB	DBpedia	YAGO	Synthetic
EJ	1.711	2.286	2.017	2.111	1.929	2.221	1.516
PJ	1.545	1.856	1.803	1.746	1.735	2.219	1.101
SIM-TD	0.451	0.716	0.659	0.582	0.511	0.674	0.325
Neo4j	0.576	0.885	0.617	0.594	0.686	0.639	0.513
DualSim	0.056	0.083	0.054	0.069	0.059	0.095	0.051
NeuroMatch	0.005	0.029	0.007	0.006	0.012	0.022	0.017
D2Match	0.039	OOM	0.045	0.038	OOM	OOM	0.040
DMPNN	0.016	0.058	0.015	0.011	0.026	0.051	0.035
HFrame	0.012	0.048	0.013	0.014	0.019	0.039	0.034
HFrameWS	0.005	0.030	0.007	0.006	0.012	0.028	0.024
HFrame _{MS}	0.012	0.046	0.013	0.014	0.019	0.039	0.023
HFrame _{WD}	0.012	0.044	0.012	0.013	0.019	0.039	0.024
HFrame _{WN}	0.013	0.048	0.013	0.014	0.019	0.040	0.024
HFrame _{WC}	0.012	0.043	0.012	0.013	0.018	0.037	0.020
HFrame _{WG}	0.013	0.048	0.013	0.014	0.019	0.040	0.024

Experimental findings. We next report our findings.

Exp-1: Accuracy. We first evaluated the accuracy of HFrame. Since EJ, PJ, SIM-TD and Neo4j are exact algorithms, their accuracy are 1. In the following, we only compared HFrame with DualSim, NeuroMatch, D2Match and DMPNN. As shown in Table 1, (1) HFrame achieves the best performance on all graphs. On average, HFrame improves DualSim, NeuroMatch, D2Match and DMPNN by 54.67%, 18.90%, 17.02% and 16.88%, respectively. This is because HFrame (a) invokes DualSim to filter candidates, (b) adopts sets to aggregate messages, and (c) uses different message passing functions for different vertices. Model D2Match runs out of memory on Citeseer, DBpedia and YAGO, marked as OOM. (2) HFrame is practical. The accuracy of HFrame can achieve 0.921 on all graphs, while the accuracy of all ML-based solutions and DualSim are lower than 0.9. This is because HFrame is more expressive than existing solutions (see Section 4).

Exp-2: Efficiency. As shown in Table 2, (1) HFrame is faster than exact algorithms. On average, HFrame outperforms SIM-TD, EJ and PJ by 28.36×, 101.91× and 85.06×, respectively. (2) HFrame is slightly slower than NeuroMatch since HFrame calls DualSim to filter candidates, and inspects cycles. (3) Although NeuroMatch is the fastest, its accuracy is much lower than HFrame. Hence, HFrame strikes a balance between expressive power and efficiency.

For a fair comparison, we evaluate HFrame and exact algorithms SIM-TD, EJ, PJ only on positive instances. As shown in Table 3, HFrame consistently outperforms exact algorithms in efficiency. We further report the average training, inference and DualSim time for each query on CPU in Table 4. The average matching time (*i.e.*, times for inference and DualSim) of HFrame over all

Table 3: Efficiency on positive examples (Time in s/query)

Method	Citation	Citeseerx	DBLP	IMDB	DBpedia	YAGO	Synthetic
EJ	1.642	2.197	1.926	2.002	1.840	2.144	1.406
PJ	1.489	1.765	1.743	1.671	1.638	2.118	0.997
SIM-TD	0.428	0.683	0.591	0.514	0.476	0.619	0.302
HFrame	0.013	0.048	0.013	0.015	0.019	0.040	0.034

Table 4: Efficiency of HFrame on CPU

Dataset	Avg Training (s/epoch)	Avg Inference (s)	Avg DualSim (s)
Citation	0.028	0.019	0.007
Citeseerx	0.207	0.138	0.018
DBLP	0.051	0.030	0.006
IMDB	0.044	0.025	0.008
DBpedia	0.093	0.051	0.007
YAGO	0.199	0.106	0.011
Synthetic	0.119	0.079	0.010

datasets is 0.074s on CPU and 0.026s on GPU, indicating no order-of-magnitude difference.

Exp-3: Parameter sensitiveness. We next evaluated the impacts of the sizes $|Q|$ of patterns (*i.e.*, $|V_Q| + |E_Q|$), the number m of layers in HGIN, the threshold t , the dimension d of embeddings, and the average degree δ_{avg} of graphs on the performance of HFrame. We conducted experiments on dataset Citation.

Varying $|Q|$. We varied $|Q|$ from 10 to 35. As shown in Table 5, (1) when $|Q|$ increases, the accuracy of $|Q|$ decreases, as expected, since making prediction is more challenging for large patterns; and (2) HFrame becomes slower when $|Q|$ increases, as expected, since it takes more time to compute embeddings.

Varying m . We varied m from 2 to 7. As shown in Table 5, (1) when m increases, HFrame gets slower, as expected, since it takes more time to compute embeddings; and (2) the accuracy of HFrame first increases and then decreases, *i.e.*, its optimal performance achieves when $m = 5$. This is because when m is small, HFrame does not have sufficient information to make a prediction; while when m is large, HFrame cannot distinguish neighbors distant from the pivot.

Varying t . We varied the threshold t from 0.01 to 0.5. As shown in Table 5, (1) the runtime of HFrame is insensitive to t , since the threshold is used only when the embeddings of vertices have been computed; and (2) the accuracy of HFrame first increases and then decreases, and its optimal performance achieves when $t = 0.1$. This is because (a) when t is small, HFrame returns true only when it correctly makes predictions, and the recall of HFrame is low; and (b) when t is large, HFrame may return true when Q is not homomorphic to G , but its embedding is slightly larger than that of G , *i.e.*, the precision of HFrame is low.

Varying d . We varied the dimension d of embeddings from 16 to 512. We found the following. (1) HFrame gets slower as d increases, since the order-embedding space inspects each dimension of embeddings; and (2) the accuracy of HFrame first increases and then decreases, and its optimal performance achieves when $d = 64$. This is because (a) when d is small, multiple vertices can be mapped to the same embedding and the accuracy of HFrame is low; and (b) if d is large, each embedding has many values, and it is hard to ensure that the embedding of Q is smaller than that of G , even if Q is homomorphic to G .

Table 5: Parameter sensitive of HFrame

$ Q $	Acc	T(ms)	m	Acc	T(ms)	t	Acc	T(ms)	d	Acc	T(ms)	δ_{avg}	Acc	T(ms)
10	0.979	11.96	2	0.827	9.92	0.01	0.883	12.42	16	0.919	8.10	[1, 2)	0.978	30.06
15	0.970	12.25	3	0.881	10.53	0.05	0.952	12.42	32	0.930	10.59	[2, 3)	0.974	35.11
20	0.946	12.47	4	0.925	11.31	0.1	0.954	12.42	64	0.954	12.42	[3, 4)	0.963	41.69
25	0.917	12.70	5	0.954	12.42	0.2	0.901	12.42	128	0.903	20.87	[4, 5)	0.962	55.13
30	0.902	13.12	6	0.929	13.59	0.3	0.908	12.43	256	0.892	28.77	[5, 6)	0.941	72.20
35	0.884	13.51	7	0.903	14.62	0.5	0.878	12.42	512	0.758	41.26	[6, $+\infty$)	0.864	93.85

Table 6: Generalization of HFrame (Acc)

Training Data	Citation	Citeseerx	DBLP	IMDB	DBpedia	YAGO	Synthetic
Synthetic	0.821	0.892	0.874	0.872	0.853	0.824	0.974
Real-life	0.954	0.982	0.969	0.963	0.969	0.921	-

Varying δ_{avg} . We generated synthetic graphs, and grouped them based on whether their average degrees δ_{avg} are in the range $[d_1, d_2]$. Each group contains 5000 graphs. As shown in Table 5, increasing graph density slightly reduces HFrame’s accuracy and increases its running time, as expected.

Exp-4: Generalization. We next evaluated the generalization ability of HFrame by training it on synthetic graphs and testing on real-life datasets. As shown in Table 6, (1) HFrame is robust to real-life patterns, achieving the accuracy above 0.860 on all graphs, which is lower than on synthetic data (0.968), but still outperforming all baselines. (2) HFrame trained on synthetic graphs performs comparably to models trained directly on real-life data, with only a 7.45% drop in accuracy on average.

Exp-5: Ablation Study. We conducted an ablation study to evaluate the selection of framework design. We compared HFrame with the following variants: (1) HFrame_{WS}, which omits DualSim for filtering candidates for each vertex in Q ; (2) HFrame_{MS}, which uses multisets for message collection and aggregation; (3) HFrame_{WD}, that aggregates messages without distinguishing edge directions; (4) HFrame_{WN}, which skips normalization after computing embeddings; (5) HFrame_{WC}, which ignores cycle lengths in patterns when determine the message-passing functions; and (6) HFrame_{WG}, which uses a loss function without the $-\alpha$ term for the positive data and the term $\frac{1}{\text{MSG}_{01}^{k,r} - \text{MSG}_0^{k,r}}$.

As showed in Tables 1 and 2, (1) HFrame outperforms all variants, as expected. For example, on average HFrame improves HFrame_{WS}, HFrame_{MS}, HFrame_{WD}, HFrame_{WN}, HFrame_{WC} and HFrame_{WG} by 2.74%, 16.38%, 6.38%, 2.56%, 3.92% and 1.94%, respectively. (2) Filtering candidates with DualSim and using sets to store received message have the most impact on the performance of HFrame, since two distinct vertices in the pattern can be mapped to the same vertex in the graph via homomorphic mappings, and collecting message with multisets results in multiple false negative results, which degrades the performance of HFrame_{MS}. (3) All variants have similar runtime, since all optimizations (e.g., storing message using sets, and normalizing the embeddings) are efficient.

Exp-6: Applications. We show how to apply HFrame in subgraph homomorphism matching and frequent pattern mining.

Subgraph homomorphism matching. We show how to enhance the performance of exact matching algorithms using HFrame. More

Table 7: Effectiveness of HFrame in candidate filtering

Method	F1 score		Time(s)	
	Citation	DBLP	Citation	DBLP
PJ	1.000	1.000	1.681	1.926
HFrame + PJ	0.832	0.835	0.762	0.780

Table 8: Effectiveness of HFrame in frequent pattern mining

Method	1	2	3	4	5	6	7	8
SPMiner	19,207	17,168	15,605	14,688	13,854	13,320	12,838	12,727
SPMiner+HF	19,207	17,168	15,605	15,173	14,688	13,854	13,320	12,838
Exact	19,207	17,168	15,605	15,173	14,688	13,854	13,320	12,838

specifically, given a pattern Q and a graph G , we (1) first invoke DualSim to filter candidates in $C(u)$ for each pattern vertex u , (2) next remove from G all vertices that are not in $C(u)$ for any u , (3) then use HGIN to check whether there is a match for each vertex v in $C(u_1)$ of the first pattern vertex u_1 in the matching order $\mathcal{O} = (u_1, \dots, u_n)$ of Q , and (4) finally, run the exact algorithm to check the remaining vertices in $C(u_1)$. As shown in Table 7, plugging HFrame slightly reduces the accuracy of exact algorithm PJ, but significantly accelerates its computation on Citation and DBLP.

Frequent pattern mining. We demonstrate the application of HFrame in frequent pattern mining. Given a graph G , frequent pattern mining is to identify patterns Q with high support. The support of Q is defined as the number of vertices in G that match the pivot (a designated vertex) of Q . We plug HFrame in the frequent pattern mining algorithm SPMiner [82], denoted by SPMiner+HF, to estimate the support of the size-5 patterns that rank in the top 8 among all candidate patterns by supports computed by the exact algorithm. On dataset Enzyme from [82], SPMiner+HF computes the supports more accurately than SPMiner, while maintaining comparable efficiency with SPMiner (159.35s vs. 151.89s).

6 Conclusion

In this paper, we proposed a framework HFrame for the subgraph homomorphism problem by combining algorithmic solutions and ML models. We showed that HFrame is more expressive than the vanilla GNN for subgraph matching. Moreover, we also provided the first generalization error bound for the subgraph matching problem. Using real-life and synthetic graphs, we experimentally validated the efficiency and effectiveness of the proposed frameworks.

Acknowledgments

This work was supported by the National Natural Science Foundation of China (No. U24B20143 and No. 62372030).

References

- [1] 2021. Citation. <https://aminer.cn/citation>.
- [2] 2021. Citeseerx. citeseerx.ist.psu.edu.
- [3] 2021. DBLP. <https://dblp.uni-trier.de/xml/>.
- [4] 2021. DBpedia. <https://en.wikipedia.org/wiki/DBpedia>.
- [5] 2021. IMDB. <https://developer.imdb.com/non-commercial-datasets/>.
- [6] 2021. YAGO. <https://yago-knowledge.org/>.
- [7] 2023. Neo4j 5.10.0. <https://neo4j.com/>.
- [8] 2025. Wikidata: SPARQL query service/queries/examples. https://www.wikidata.org/wiki/Wikidata:SPARQL_query_service/queries/examples
- [9] Junya Arai, Yasuhiro Fujiwara, and Makoto Onizuka. 2023. GuP: Fast Subgraph Matching by Guard-based Pruning. *Proc. ACM Manag. Data* 1, 2 (2023), 167:1–167:26.
- [10] Pablo Barceló, Mikhail Galkin, Christopher Morris, and Miguel A. Romero Orth. 2022. Weisfeiler and leman go relational. In *LoG*. 46–1.
- [11] Pablo Barceló, Egor V. Kostylev, Mikael Monet, Jorge Pérez, Juan L. Reutter, and Juan Pablo Silva. 2020. The Expressive Power of Graph Neural Networks as a Query Language. *SIGMOD Rec.* 49, 2 (2020), 6–17.
- [12] Bibek Bhattacharai, Hang Liu, and H. Howie Huang. 2019. CECI: Compact Embedding Cluster Index for Scalable Subgraph Matching. In *SIGMOD*. 1447–1462.
- [13] Fei Bi, Lijun Chang, Xuemin Lin, Lu Qin, and Wenjie Zhang. 2016. Efficient Subgraph Matching by Postponing Cartesian Products. In *SIGMOD*. ACM, 1199–1214.
- [14] Vincenzo Bonnici, Rosalba Giugno, Alfredo Pulvirenti, Dennis E. Shasha, and Alfredo Ferro. 2013. A subgraph isomorphism algorithm and its application to biochemical data. *BMC Bioinformatic* 14, S-7 (2013), S13.
- [15] Giorgos Bouritsas, Fabrizio Frasca, Stefanos Zafeiriou, and Michael M Bronstein. 2022. Improving graph neural network expressivity via subgraph isomorphism counting. *IEEE Trans. Pattern Anal. Mach. Intell.* 45, 1 (2022), 657–668.
- [16] Joel Brynielsson, Johanna Höglberg, Lisa Kaati, Christian Mårtenson, and Pontus Svensson. 2010. Detecting social positions using simulation. In *ASONAM*. 48–55.
- [17] Jin-yi Cai, Martin Fürer, and Neil Immerman. 1992. An optimal lower bound on the number of variables for graph identification. *Comb.* 12, 4 (1992), 389–410.
- [18] Vincenzo Carletti, Pasquale Foggia, Antonio Greco, Mario Vento, and Vincenzo Vigilante. 2019. VF3-light: A lightweight subgraph isomorphism algorithm and its experimental evaluation. *Pattern Recognition Letters* 125 (2019), 591–596.
- [19] Vincenzo Carletti, Pasquale Foggia, Alessia Saggesse, and Mario Vento. 2017. Introducing VF3: A new algorithm for subgraph isomorphism. In *GrRPR*. 128–139.
- [20] Jiazhou Chen, Hong Peng, Guoqiang Han, Hongmin Cai, and Jialun Cai. 2019. HOGMMNC: a higher order graph matching with multiple network constraints model for gene–drug regulatory modules identification. *Bioinformatics* 35, 4 (2019), 602–610.
- [21] Jiefeng Cheng, Jeffrey Xu Yu, and S Yu Philip. 2010. Graph pattern matching: A join/semijoin approach. *TKDE* 23, 7 (2010), 1006–1021.
- [22] Jiefeng Cheng, Xianggang Zeng, and Jeffrey Xu Yu. 2013. Top-k graph pattern matching over large graphs. In *ICDE*. 1033–1044.
- [23] Stephen A Cook. 2023. The complexity of theorem-proving procedures. In *Logic, Automata, and Computational Complexity: The Works of Stephen A. Cook*. 143–152.
- [24] Nikola Dragovic, Cem Okulmus, and Magdalena Ortiz. 2023. Rewriting Ontology-Mediated Navigational Queries into Cypher. In *DL*, Vol. 3515.
- [25] Ruihui Du, Jiannan Yang, Yongzhi Cao, and Hanpin Wang. 2018. Personalized graph pattern matching via limited simulation. *Knowledge-Based Systems* 141 (2018), 31–43.
- [26] Sourav Dutta, Pratik Nayek, and Arnab Bhattacharya. 2017. Neighbor-aware search for approximate labeled graph matching using the chi-square statistics. In *WWW*. 1281–1290.
- [27] Wenfei Fan, Jianzhong Li, Shuai Ma, Nan Tang, Yinghui Wu, and Yunpeng Wu. 2010. Graph pattern matching: From intractable to polynomial time. *Proceedings of the VLDB Endowment* 3, 1-2 (2010), 264–275.
- [28] Wenfei Fan, Jianzhong Li, Shuai Ma, Hongzhi Wang, and Yinghui Wu. 2010. Graph homomorphism revisited for graph matching. *Proc. VLDB Endow.* 3, 1 (2010), 1161–1172.
- [29] Wenfei Fan, Kehan Pang, Ping Lu, and Chao Tian. 2024. Making It Tractable to Detect and Correct Errors in Graphs. *TODS* 49, 4 (2024), 16:1–16:75.
- [30] Wenfei Fan, Xin Wang, and Yinghui Wu. 2013. ExpFinder: Finding experts by graph pattern matching. In *ICDE*. 1316–1319.
- [31] Wenfei Fan, Xin Wang, and Yinghui Wu. 2013. Incremental graph pattern matching. *TODS* 38, 3 (2013), 1–47.
- [32] Wenfei Fan, Xin Wang, Yinghui Wu, and Dong Deng. 2014. Distributed graph simulation: Impossibility and possibility. *Proc. VLDB Endow.* 7, 12 (2014), 1083–1094.
- [33] Arash Fard, M Usman Nisar, John A Miller, and Lakshmin Ramaswamy. 2014. Distributed and scalable graph pattern matching: Models and algorithms. *IJBD* 1, 1 (2014), 1–14.
- [34] Jiarui Feng, Yixin Chen, Fuhai Li, Anindya Sarkar, and Muhan Zhang. 2022. How powerful are k-hop message passing graph neural networks. *NeurIPS* 35 (2022), 4776–4790.
- [35] Jianliang Gao, Ping Liu, Xuedan Kang, Lixia Zhang, and Jianxin Wang. 2016. PRS: parallel relaxation simulation for massive graphs. *Comput. J.* 59, 6 (2016), 848–860.
- [36] Vikas K. Garg, Stefanie Jegelka, and Tommi S. Jaakkola. 2020. Generalization and Representational Limits of Graph Neural Networks. In *ICML*, Vol. 119. 3419–3430.
- [37] Floris Geerts and Juan L. Reutter. 2022. Expressiveness and Approximation Properties of Graph Neural Networks. *ICLR* (2022).
- [38] Floris Geerts, Jasper Steegmans, and Jan Van den Bussche. 2022. On the Expressive Power of Message-Passing Neural Networks as Global Feature Map Transformers. In *FoIKS*, Vol. 13388. 20–34.
- [39] Martin Grohe. 2023. The Descriptive Complexity of Graph Neural Networks. In *LICS*. 1–14.
- [40] William L. Hamilton, Zhitao Ying, and Jure Leskovec. 2017. Inductive Representation Learning on Large Graphs. In *NIPS*. 1024–1034.
- [41] Myoungji Han, Hyunjoon Kim, Geonmo Gu, Kunsoo Park, and Wook-Shin Han. 2019. Efficient Subgraph Matching: Harmonizing Dynamic Programming, Adaptive Matching Order, and Failing Set Together. In *SIGMOD*. 1429–1446.
- [42] Wook-Shin Han, Jinsoo Lee, and Jeong-Hoon Lee. 2013. Turboiso: towards ultrafast and robust subgraph isomorphism search in large graph databases. In *SIGMOD*. 337–348.
- [43] Mengyue Hang, Jennifer Neville, and Bruno Ribeiro. 2021. A Collective Learning Framework to Boost GNN Expressiveness for Node Classification. In *ICML*, Vol. 139. 4040–4050.
- [44] Huahai He and Ambuj K. Singh. 2008. Graphs-at-a-time: query language and access methods for graph databases. In *SIGMOD*. ACM, 405–418.
- [45] Arjit Khan, Yinghui Wu, Charu C Aggarwal, and Xifeng Yan. 2013. Nema: Fast graph search with label similarity. *Proc. VLDB Endow.* 6, 3 (2013), 181–192.
- [46] Hyunjoon Kim, Yunyoung Choi, Kunsoo Park, Xuemin Lin, Seok-Hee Hong, and Wook-Shin Han. 2021. Versatile Equivalences: Speeding up Subgraph Query Processing and Subgraph Matching. In *SIGMOD*. 925–937.
- [47] Zixun Lan, Limin Yu, Linglong Yuan, Zili Wu, Qiang Niu, and Fei Ma. 2023. Sub-GMN: The Neural Subgraph Matching Network Model. In *CISP-BMEI*. 1–7.
- [48] Zixuan Li, Zhongni Hou, Saiping Guan, Xiaolong Jin, Weihua Peng, Long Bai, Yajuan Lyu, Wei Li, Jiafeng Guo, and Xueqi Cheng. 2022. Hismatch: Historical structure matching based temporal knowledge graph reasoning. *arXiv preprint arXiv:2210.09708* (2022).
- [49] Nicola Licheri, Vincenzo Bonnici, Marco Beccuti, and Rosalba Giugno. 2021. GRAPES-DD: exploiting decision diagrams for index-driven search in biological graph databases. *BMC bioinformatics* 22 (2021), 1–24.
- [50] Xin Liu and Yangqiu Song. 2022. Graph Convolutional Networks with Dual Message Passing for Subgraph Isomorphism Counting and Matching. In *AAAI*. 7594–7602.
- [51] Xuanzhou Liu, Lin Zhang, Jiaqi Sun, Yujiu Yang, and Haiqin Yang. 2023. D2Match: Leveraging Deep Learning and Degeneracy for Subgraph Matching. In *ICML*, Vol. 202. 22454–22472.
- [52] Shuai Ma, Yang Cao, Wenfei Fan, Jinpeng Huai, and Tianyu Wo. 2011. Capturing topology in graph pattern matching. *Proc. VLDB Endow.* 5, 4 (2011), 310–321.
- [53] Shuai Ma, Yang Cao, Wenfei Fan, Jinpeng Huai, and Tianyu Wo. 2014. Strong simulation: Capturing topology in graph pattern matching. *TODS* 39, 1 (2014), 4:1–4:46.
- [54] Haggai Maron, Heli Ben-Hamu, Nadav Shamir, and Yaron Lipman. 2019. Invariant and equivariant graph networks. *ICLR* (2019).
- [55] Christopher Morris, Floris Geerts, Jan Tönnhoff, and Martin Grohe. 2023. WL meet VC. In *ICML*, Vol. 202. 25275–25302.
- [56] Christopher Morris, Martin Ritzert, Matthias Fey, William L Hamilton, Jan Eric Lenssen, Gaurav Rattan, and Martin Grohe. 2019. Weisfeiler and leman go neural: Higher-order graph neural networks. In *AAAI*, Vol. 33. 4602–4609.
- [57] Peng Peng, Shengyi Ji, M. Tamer Özsu, and Lei Zou. 2024. Minimum motif-cut: a workload-aware RDF graph partitioning strategy. *VLDB J.* 33, 5 (2024), 1517–1542.
- [58] Indradymuna Roy, Venkata Sai Baba Reddy Velugoti, Soumen Chakrabarti, and Abir De. 2022. Interpretable Neural Subgraph Matching for Graph Retrieval. In *AAAI*. 8115–8123.
- [59] Franco Scarselli, Marco Gori, Ah Chung Tsoi, Markus Hagenbuchner, and Gabriele Monfardini. 2008. The graph neural network model. *IEEE transactions on neural networks* 20, 1 (2008), 61–80.
- [60] Michael Sejr Schlichtkrull, Thomas N. Kipf, Peter Bloem, Rianne van den Berg, Ivan Titov, and Max Welling. 2018. Modeling Relational Data with Graph Convolutional Networks. In *ESWC*, Vol. 10843. 593–607.
- [61] Kartik Sharma, Yeon-Chang Lee, Sivagami Nambi, Aditya Salian, Shlok Shah, Sang-Wook Kim, and Srijan Kumar. 2024. A Survey of Graph Neural Networks for Social Recommender Systems. *ACM Comput. Surv.* 56, 10 (2024), 265.
- [62] Qun Shi, Guanfeng Liu, Kai Zheng, An Liu, Zhiyu Li, Lei Zhao, and Xiaofang Zhou. 2017. Multi-constrained top-K graph pattern matching in contextual social graphs. In *ICWS*. 588–595.
- [63] Shixuan Sun and Qiong Luo. 2019. Scaling up subgraph query processing with efficient subgraph matching. In *ICDE*. 220–231.
- [64] Shixuan Sun and Qiong Luo. 2020. Subgraph matching with effective matching order and indexing. *TKDE* 34, 1 (2020), 491–505.
- [65] Shixuan Sun, Xibo Sun, Yulin Che, Qiong Luo, and Bingsheng He. 2020. RapidMatch: A Holistic Approach to Subgraph Query Processing. *Proc. VLDB Endow.* 14, 2 (2020), 176–188.

[66] Komal Teru, Etienne Denis, and Will Hamilton. 2020. Inductive relation prediction by subgraph reasoning. In *International Conference on Machine Learning*. PMLR, 9448–9457.

[67] Yuanyuan Tian, Richard C Mceachin, Carlos Santos, David J States, and Jignesh M Patel. 2007. SAGA: a subgraph matching tool for biological graphs. *Bioinformatics* 23, 2 (2007), 232–239.

[68] Julian R. Ullmann. 1976. An Algorithm for Subgraph Isomorphism. *J. ACM* 23, 1 (1976), 31–42.

[69] Ivan Vendrov, Ryan Kiros, Sanja Fidler, and Raquel Urtasun. 2016. Order-Embeddings of Images and Language. In *ICLR*.

[70] Haorui Wang, Haotao Yin, Muhan Zhang, and Pan Li. 2022. Equivariant and stable positional encoding for more powerful graph neural networks. *ICLR* (2022).

[71] Yanling Wang, Jing Zhang, Shasha Guo, Hongzhi Yin, Cuiping Li, and Hong Chen. 2021. Decoupling Representation Learning and Classification for GNN-based Anomaly Detection. In *SIGIR*. 1239–1248.

[72] Zhaohui Wang, Qi Cao, Huawei Shen, Bingbing Xu, and Xueqi Cheng. 2022. Twin Weisfeiler-Lehman High Expressive GNNs for Graph Classification. *arXiv preprint arXiv:2203.11683* (2022).

[73] Zhiyang Wang, Juan Cerviño, and Alejandro Ribeiro. 2024. Generalization of Geometric Graph Neural Networks. *CoRR* abs/2409.05191 (2024).

[74] Boris Weisfeiler and Andrei Leman. 1968. The reduction of a graph to canonical form and the algebra which appears therein. *nti, Series 2*, 9 (1968), 12–16.

[75] Xiaoying Wu, Dimitri Theodoratos, Dimitrios Skoutas, and Michael Lan. 2023. A novel framework for the efficient evaluation of hybrid tree-pattern queries on large data graphs. *Information Systems* 117 (2023), 102249.

[76] Yinghui Wu, Shengqi Yang, and Xifeng Yan. 2013. Ontology-based subgraph querying. In *ICDE*. 697–708.

[77] Keyulu Xu, Weihua Hu, Jure Leskovec, and Stefanie Jegelka. 2019. How powerful are graph neural networks? *ICLR* (2019).

[78] Kun Xu, Liwei Wang, Mo Yu, Yansong Feng, Yan Song, Zhiguo Wang, and Dong Yu. 2019. Cross-lingual knowledge graph alignment via graph matching neural network. *arXiv preprint arXiv:1905.11605* (2019).

[79] Xifeng Yan, Philip S Yu, and Jiawei Han. 2004. Graph indexing: a frequent structure-based approach. In *SIGMOD*. 335–346.

[80] Rongjian Yang, Zhijie Zhang, Weiguo Zheng, and Jeffrey Xu Yu. 2023. Fast Continuous Subgraph Matching over Streaming Graphs via Backtracking Reduction. *Proc. ACM Manag. Data* 1, 1 (2023), 15:1–15:26.

[81] Yutong Ye, Xiang Lian, and Mingsong Chen. 2024. Efficient Exact Subgraph Matching via GNN-based Path Dominance Embedding. *Proc. VLDB Endow.* 17, 7 (2024), 1628–1641.

[82] Rex Ying, Tianyu Fu, Andrew Wang, Jiaxuan You, Yu Wang, and Jure Leskovec. 2024. Representation Learning for Frequent Subgraph Mining. *arXiv preprint arXiv:2402.14367* (2024).

[83] Rex Ying, Zhaoyu Lou, Jiaxuan You, Chengtao Wen, Arquimedes Canedo, and Jure Leskovec. 2020. Neural Subgraph Matching. *CoRR* abs/2007.03092 (2020). <https://arxiv.org/abs/2007.03092>

[84] Jiaxuan You, Jonathan M Gomes-Selman, Rex Ying, and Jure Leskovec. 2021. Identity-aware graph neural networks. In *AAAI*, Vol. 35. 10737–10745.

[85] Ye Yuan, Guoren Wang, Haixun Wang, and Lei Chen. 2011. Efficient subgraph search over large uncertain graphs. *Proc. VLDB Endow.* 4, 11 (2011), 876–886.

[86] Bingxu Zhang, Changjun Fan, Shixuan Liu, Kuihua Huang, Xiang Zhao, Jincai Huang, and Zhong Liu. 2023. The expressive power of graph neural networks: A survey. *arXiv preprint arXiv:2308.08235* (2023).

[87] Bohang Zhang, Shengjie Luo, Liwei Wang, and Di He. 2023. Rethinking the Expressive Power of GNNs via Graph Biconnectivity. In *ICLR*.

[88] Tianming Zhang, Xinwei Cai, Lu Chen, Zhengyi Yang, Yunjun Gao, Bin Cao, and Jing Fan. 2024. Towards efficient simulation-based constrained temporal graph pattern matching. *World Wide Web (WWW)* 27, 3 (2024), 22.

[89] Ziwei Zhang, Peng Cui, Jian Pei, Xin Wang, and Wenwu Zhu. 2021. Eigen-gnn: A graph structure preserving plug-in for gnn. *TKDE* 35, 3 (2021), 2544–2555.

[90] Zhijie Zhang, Yujie Lu, Weiguo Zheng, and Xuemin Lin. 2024. A Comprehensive Survey and Experimental Study of Subgraph Matching: Trends, Unbiasedness, and Interaction. *Proc. ACM Manag. Data* 2, 1 (2024), 60:1–60:29.

[91] Peixiang Zhao, Jeffrey Xu Yu, and Philip S Yu. 2007. Graph indexing: tree + delta \geq graph. In *VLDB*. 938–949.

[92] Xiang Zhao, Chuan Xiao, Xuemin Lin, Qing Liu, and Wenjie Zhang. 2013. A partition-based approach to structure similarity search. *Proc. VLDB Endow.* 7, 3 (2013), 169–180.

A Appendix

A.1 Proof of Theorem 4.1

Assume by contradiction that there exist a pattern Q , a graph G , a vertex u in Q and a vertex v in G such that HGIN^v returns false,

but DualSim returns true, *i.e.*, (u, v) exists in the relation $S_{(Q, G)}$ computed by DualSim. We deduce a contradiction by analyzing the computation of HGIN^v . Observe that (a) computing embeddings of u and v can be represented by trees of height m , where m is the number of layers in HGIN^v ([36]; see Figures 5(a) and 5(b) for an example); and (b) vertex v may have more adjacent edges in G than u , *e.g.*, paths colored in red in Figure 5(b). When HGIN^v returns false, the embedding of v is not larger than that of u (see Section 3). Because all functions $\text{MSG}^{k,r}$ and AGG^k ($k \in \mathcal{L}$) in HGIN^v are injective and monotonic, there exists a path p_0 in the tree representing the computation of embedding of u (*e.g.*, the path colored in blue in Figure 5(a)), such that no path from v carries the same labels as p_0 . However, if this holds, DualSim can also identify such path and returns false. Indeed, the computation of DualSim can also be represented as a tree (see Figures 5(c) for an example). The match relation $S_{(Q, G)}$ can be constructed from common parts of trees roots at u and v (see Section 2). When such a path p_0 exists in G , DualSim can also identify that p_0 is missed in the tree of v , and (u, v) is not contained in $S_{(Q, G)}$, *i.e.*, DualSim returns false, a contradiction.

A.2 Proof of Theorem 4.2

(1) We first show that given a pattern Q , a graph G , a vertex u in Q and a vertex v in G , if $(u, v) \notin S_{(Q, G)}$, then there exists a HGIN that returns false given the input. Indeed, when $(u, v) \notin S_{(Q, G)}$, there exists a path p from u in Q such that p is not a path from v in G . Then we can construct a HGIN such that it has $|p|$ layers, and all its functions $\text{MSG}^{k,r}$ and AGG^k ($k \leq |p|$) are injective and monotonic. Then the embedding of u computed by HGIN is not smaller than that of v , *i.e.*, HGIN returns false, since the embedding of p is used to compute the embedding of u but not in that of v , and functions $\text{MSG}^{k,r}$ and AGG^k ($k \leq |p|$) in HGIN are injective and monotonic.

(2) We next show that HGIN is more expressive than DualSim. Consider graphs G_2 and G_3 in Figure 1, which are extended from [84]. We can verify that there does not exist a homomorphic mapping from G_3 to G_2 , since G_3 contains triangles (*i.e.*, the subgraph induced by w_1, w_5 and w_6), while G_2 does not. We next show that given G_3, G_2, v_1 and w_1 , (1) HGIN returns false but (2) $(v_1, w_1) \in S_{(G_3, G_2)}$. If these hold, then HGIN is more expressive than DualSim, *i.e.*, HGIN can distinct more non-homomorphic graphs.

(I) We first prove that HGIN returns false. This is because (a) v_1 is contained in a cycle C of length 3, while w_1 does not; (b) HGIN ensures that $\text{MSG}_1^{k,r}$ is sufficiently larger than $\text{MSG}_0^{k,r}$; and (c) the cycle C ensures that computing the embedding of v_1 invokes more $\text{MSG}_1^{k,r}$, which leads to the embedding of v_1 being larger than that of w_1 . Consider two trees in Figure 6, which represent the computation of embeddings of v_1 and w_1 . The vertices with message passing function $\text{MSG}_1^{k,r}$ are marked red. We can see that the computation of embedding of v_1 invokes more times of function $\text{MSG}_1^{k,r}$ than the computation of embedding of w_1 .

(II) We next show that $(v_1, w_1) \in S_{(G_3, G_2)}$. That is, (v_1, w_1) exists in the dual simulation of G_3 and G_2 . Observe that both G_3 and G_2 are regular, and all vertices have the same number of neighbors. Therefore, all vertices pairs exist in $V_{G_3} \times V_{G_2}$, *i.e.*, $S_{(G_3, G_2)} = V_{G_3} \times V_{G_2}$.

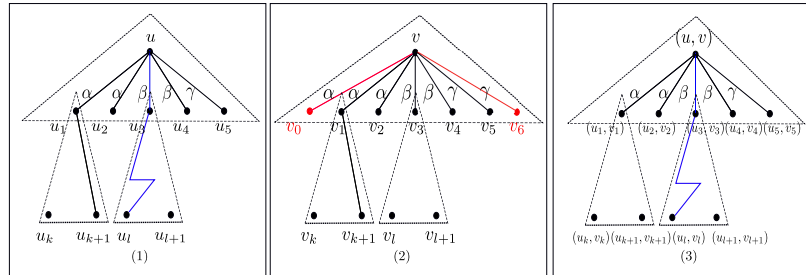


Figure 5: Computation of embeddings and DualSim

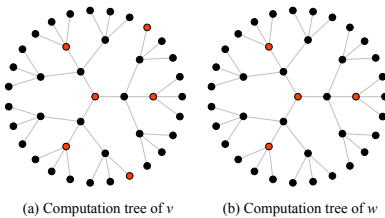


Figure 6: Computation trees of embeddings

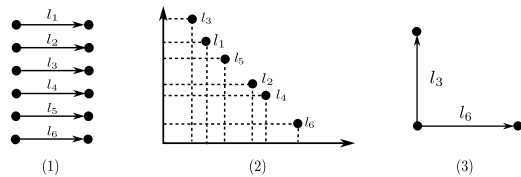


Figure 7: Example in Theorem 4.3

A3. Proof of Theorem 4.3

Assume that the embeddings are finite dimension, and let the embedding be d -dimension. We select $2d$ distinct edge labels l_1, \dots, l_{2d} , which embeddings are e_1, \dots, e_{2d} , respectively. Since the embeddings are d -dimension, we can pick d embeddings e'_1, \dots, e'_d such that the i -th index of e'_i is maximum among all $2d$ embeddings e_1, \dots, e_{2d} . Let l'_1, \dots, l'_d be the labels with embeddings e'_1, \dots, e'_d , respectively. Next we construct a star pattern Q_s with d edges adjacent to the same vertex, where the edge labels are the picked d labels l'_1, \dots, l'_d . We can deduce a contradiction by comparing the embeddings of Q_s and that of all these $2d$ labels. (1) Because Q_s consists of d edge labels, the embedding of Q_s must be larger than the embeddings of these d labels, based on the order-embedding space (see the prediction function of HGIN); (2) each of these d vectors has the maximum value for at least one index, then the embedding of Q_s must be larger than the embeddings of all $2d$ labels, which is a contradiction, since Q_s has only d labels, and l_1, \dots, l_{2d} are distinct.

Consider the six edges in Figure 7(1), which carry distinct labels l_1, \dots, l_6 . Their embeddings in two-dimensional space as shown in Figure 7(b). Since these labels are distinct, none of these labels is homomorphic to any of the other labels. Therefore, given any embeddings $e_1 = (a_1, a_2)$ and $e_2 = (b_1, b_2)$ of two labels l_1 and l_2 , respectively, if $a_1 \leq b_1$, then $a_2 > b_2$; and if $a_2 \leq b_2$, then $a_1 > b_1$ (see Figure 7(2)). Then we pick two labels l_3 and l_6 , which have the largest

values in the second dimension and the first dimension, respectively, and construct a pattern Q_s in Figure 7(3). We can verify that (I) Q_s is homomorphic to none of the edges in Figure 7(1). (II) Since l_3 and l_6 have the largest values in the second dimension and the first dimension, respectively, the embedding of Q_s is larger than embeddings of all edges in Figure 7(1), *i.e.*, the six edges in Figure 7(1) can be homomorphic to Q_s , which contradicts the fact that l_1, \dots, l_6 are distinct.

A4. Proof of Theorem 4.4

We establish the Rademacher complexity of HFrame by extending the proof of the Rademacher complexity for GNNs [36]. Since DualSim does not have any parameters, and works for any inputs, we only bound the Rademacher complexity of HGIN. We prove the bound in five steps: (1) represent the computation of HGIN by a tree; (2) quantify the impact of change of parameters on the embeddings; (3) bound the changes in prediction probability; (4) bound the covering numbers for HGIN; and (5) bound the Rademacher complexity using the covering numbers. We omit the details due to page limits.

A5. Complex queries

For complex queries with multiple cycles and a large number of vertices, exact algorithms can be slow and HFrame is much faster than them. Given a query with 55 vertices (Figure 8) extracted from Citeseerx, SIM-TD, PJ and EJ took 1.138s, 6.279s and over 30 seconds, respectively, to conduct the query over an extracted subgraph with 1146 vertices and 2176 edges, while HFrame took only 0.074s.

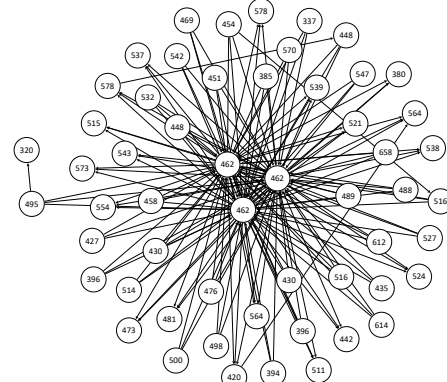


Figure 8: Example of complex query